Fermi National Accelerator Laboratory

FERMILAB-Pub-77/51-THY
June 1977

# Statistical Mechanics of a (1 + 1)-Dimensional Quantum Field Theory at Finite Density and Temperature

H. B. THACKER
Fermi National Accelerator Laboratory, Batavia, Illinois 60510

## ABSTRACT

The quantum field theory in one space + one time dimension described by the Lagrangian $\mathscr{L} = i/2\ \phi^* \overleftrightarrow{\partial_0}\ \phi - (\partial_1\ \phi^*)(\partial_1\ \phi) - c\ |\phi|^4$ is studied for systems with finite temperature and particle density. Using momentum space techniques previously developed, a graphical procedure is obtained for calculating inner products of many-particle scattering state wave functions. The unitarity of the wave operator $U(0, -\infty)$ is demonstrated as a pattern of graphical cancellations. An operator formulation of statistical mechanics is derived in which partition functions are given in terms of matrix elements having the form of diagonal (forward) inner products. The importance of non-commutativity of the forward limit and the $i\epsilon \to 0$ limit is noted and traced to the presence of forward singular graphs in the inner product. Combining this observation with wave operator unitarity, we obtain a graphical recipe for calculating N-body partition functions. The thermodynamics first described by Yang and Yang is obtained by summation of the fugacity series for the grand partition function.

Operated by Universities Research Association Inc. under contract with the Energy Research and Development Administration

## I. INTRODUCTION

This paper is the third in a series[1,2] dealing with the quantum field theory in one space plus one time dimension described by the Lagrangian

$$\mathscr{L} = \tfrac{1}{2} i \phi^* \overleftrightarrow{\partial_0} \phi - (\partial_1 \phi^*)(\partial_1 \phi) - c \phi^* \phi^* \phi \phi \tag{1.1}$$

where $\phi(x)$ is a complex scalar boson field. In this paper we consider only the repulsive case $c > 0$. Previous treatments[3-8] of this model have begun with the first-quantized counterpart of (1.1), which is a set of N-body (N = 1, 2, ...) Schroedinger equations with a two-body $\delta$-function interaction.[9] Many-body wave functions of the form first suggested by Bethe[10] provide the basic dynamical input in these discussions. Our approach differs essentially from others in that we work directly from the quantum field theory (1.1), relying primarily on graphical momentum space techniques. The graphical formalism that emerges is appealing in its simplicity and clarity of physical interpretation (see Sec. IV of II). It provides a complete description of the "zero density" phenomena (scattering theory) associated with (1.1).

The present paper extends the results of II to deal with many-particle systems at finite density and temperature. The main result is a graphical description of the equation of state. The integral equation of Yang and Yang[6] follows from an inspection of quasiparticle self-energy graphs. In Sec. II we review the relevant results from the scattering theory of N-body systems developed in II. In Sec. III the graphical representation of N-body scattering

state wave functions is used to study the orthonormality of these functions or, equivalently, to investigate the unitarity of the wave operator $U(0, -\infty)$. The cancellations among various terms of an inner product, enforced by wave operator unitarity, are a crucial ingredient in our calculation of thermodynamic quantities. Sec. IV describes an operator formulation of statistical mechanics which was developed specifically to treat this model but may be of more general interest. It is similar in spirit to the work of Goldberger[11] and of Dashen et al.,[12-13] but differs substantially from both in that the matrix elements which must be computed are not those of a (formal) phase shift operator, but rather of a (formal) inner product of wave operators, specifically, matrix elements of $\Omega^\dagger\Omega$ where $\Omega$ is similar to the wave operator $U(0, -\infty)$. The difference between $\Omega$ and $U(0, -\infty)$ lies in the prescription for calculating diagonal (forward) matrix elements, i.e. the order in which the $i\epsilon \to 0$ and $k_i' \to k_i$ limits are taken. By considering the unitarity of the wave operator $U(0, -\infty)$, our attention is focussed on the forward singularities which prevent these limits from being interchanged. The graphical formalism is very helpful here since the momentum space singularities of a term in the inner product are a direct reflection of the structure of the corresponding graph. There emerges from this study a graphical method for calculating forward matrix elements of $\Omega^\dagger\Omega$. In Sec. V this method is used to calculate partition functions. The fugacity series for the grand partition function is explicitly summed in terms of a one-particle self-energy function $\pi(k)$. The graphical expansion for $\pi(k)$

can be written as an integral equation. This reproduces the thermodynamics previously derived by a variational method using Bethe's hypothesis.[6]

## II. REVIEW OF MANY-BODY SCATTERING THEORY

We review here the scattering theory results from I and II which will be relevant to the discussion of finite density systems. The graphical description of the thermal equilibrium state presented in Sec. V is an outgrowth of the "factorized graph" representation of many body scattering state wave functions derived in II. An N-body in-state wave function is constructed from a free N-particle plane wave $|k_1 k_2 \ldots k_N\rangle \equiv |k\rangle$ by a perturbative expansion of the Lippmann-Schwinger equation,

$$|\Psi_N^{(+)}(k)\rangle = U(0, -\infty)\,|k\rangle = \sum_{n=0}^{\infty} \left[G_0(\omega_k)V\right]^n |k\rangle \qquad (2.1)$$

where $G_o$ is the free particle Green's function operator

$$G_0(\omega) = \frac{1}{\omega - H_0 + i\epsilon} \qquad (2.2)$$

and $\omega_k$ is the energy of the plane wave,

$$\omega_k = \sum_{i=1}^{N} k_i^2 \quad . \qquad (2.3)$$

The order-by-order calculation of (2.1) can be represented by a set of graphs containing $|\phi|^4$ Feynman vertices, energy denominators, and loop

integrations. In II it was shown that, by judicious dissection and recombination of these graphs, the perturbation theory of the many body wave function (2.1) can be reduced to an equivalent set of "factorized" graphs.

A factorized N-body wave function graph consists of N solid vertical lines with some number of directed wiggly exchange lines passing between them. An example is shown in Fig. 1. The solid lines, representing the particles in the system, proceed from the bottom to the top of the graph without direct intersection (in contrast to the original Feynman graphs). In anticipation of their role in finite density calculations, we will refer to these solid lines as quasiparticle lines. Each quasiparticle line can be separately and unambiguously traced through the graph, and hence, at any point in the graph a quasiparticle may be identified by the momentum which it had in the initial state. Here it is important to understand the rather different roles played by the initial state momentum variables $k_i$ and the final state momentum variables $p_i$ in the graphs for the in state wave function $\langle p | \Psi_N^{(+)}(k) \rangle$. The $p_i$'s are Fourier conjugate to the particle positions at $t = 0$ and thus reflect the actual momentum content of the interacting system. The $k_i$'s (sometimes called the pseudomomentum variables in the literature on Bethe's hypothesis) serve as labels for the set of in state wave functions.

A wiggly exchange line which connects quasiparticle lines of pseudomomentum $k_i$ and $k_j$, with $k_i < k_j$, represents the product of a k-dependent "coupling constant" $ic/(k_i - k_j)$ and a momentum pole $(-i)/(q - i\epsilon)$

where q is the momentum carried by the wiggly line. It is interesting that the forward singularities (poles at zero momentum transfer) represented by these lines are of the same type as those studied by Landau in the theory of repulsive Fermi systems.[14] Landau showed that these singularities could be associated with a collective excitation of quasiparticles known as "zero sound." Drawing on this analogy, we will refer to the wiggly lines in a factorized graph as phonon lines. (We do not attempt to justify this terminology in the present context but adopt it as a convenience. Discussion of the physical excitation spectrum for finite density systems described by (1.1) will be deferred to a future publication.)

The perturbation theory rules for calculating factorized graphs were stated in Eq. (2.5) of II. There it was shown that each graph could be written as a skeleton multiplied by a dressing function which depends only on the $k_i$'s. By reordering the phonon lines (which leaves the value of the graph unchanged) and carrying out loop integrations, each skeleton can be reduced to one of a standard set of $2^{N(N-1)/2}$ N-body skeletons. $\mathscr{K}_N(p, k; \mathscr{C})$. Thus, for example, Fig. 2a is reduced to Fig. 2b. For a given set of pseudomomenta $k_1, \ldots k_N$, a skeleton is completely specified by a set of pairs $\mathscr{C}$, to be called a "collision set," which lists those pairs of quasiparticles that interacted. For example, Fig. 2 is described by the collision set $\{(1, 2), (2, 3)\}$. If we define a set of $N(N-1)/2$ pairs,

$$\mathscr{E}_N = \{(i, j) \,|\, i < j \leq N\} \quad , \tag{2.4}$$

then $\mathscr{C}$ can be any subset of $\mathscr{E}_N$ (including, of course, the empty set and $\mathscr{E}_N$ itself). Equivalently, $\mathscr{C} \in \mathscr{P}(\mathscr{E}_N)$ where $\mathscr{P}(\mathscr{E}_N)$ is the power set (set of all subsets) of $\mathscr{E}_N$. The full dressing function $\tilde{\mathscr{D}}(\mathscr{C})$ for a skeleton $\mathscr{K}(\mathscr{C})$ (summed to all orders) contains a factor (assuming $k_i < k_j$

$$\tau(k_i - k_j) = \frac{2ic}{k_i - k_j - ic} , \tag{2.5}$$

for each element (i, j) of the collision set $\mathscr{C}$ (c.f. Eq. (4.5) of II). Following this procedure, we obtain the skeleton expansion for the N-body wave function

$$\langle p | \Psi_N^{(+)}(k) \rangle = (2\pi)\delta\left(\sum_{i=1}^{N} p - \sum_{i=1}^{N} k\right) \sum_{\mathscr{C} \in \mathscr{P}(\mathscr{E}_N)} \tilde{\mathscr{K}}_N(p, k; \mathscr{C}) \tag{2.6}$$

where $\tilde{\mathscr{K}}_N(p, k; \mathscr{C})$ is a dressed skeleton,

$$\tilde{\mathscr{K}}_N(p, k; \mathscr{C}) = \mathscr{K}_N(p, k; \mathscr{C}) \prod_{(i,j) \in \mathscr{C}} \tau(k_{ij}) . \tag{2.7}$$

In (2.7) and elsewhere we use a double subscript notation for momentum differences,

$$k_{ij} \equiv k_i - k_j . \tag{2.8}$$

$\mathscr{K}_N(p, k; \mathscr{C})$ is computed from rules (2.5a) and (2.5c) of II. Here we will state the rules for directly computing a dressed skeleton $\tilde{\mathscr{K}}_N(p, k; \mathscr{C})$.

The necessity for specifying a particular ordering of the pseudomomentum variables (c.f. Eq. (2.4) of II) can be eliminated by introducing a symmetrized "phonon propagator,"

$$\tilde{\Delta}(q;\, k - k') = \tau(k' - k)\,\frac{-i}{q - i\epsilon} \qquad k > k'$$

$$= \tau(k - k')\,\frac{i}{q + i\epsilon} \qquad k < k' \quad . \tag{2.9}$$

Note that $\tilde{\Delta}(q;\, k - k') = \tilde{\Delta}(-q;\, k' - k)$ and thus the sense of q can be defined in either direction. A dressed skeleton graph $\tilde{\mathscr{K}}(p,\, k;\, \mathscr{E})$ is given by the following rules:

(a) A propagator $\tilde{\Delta}(q;\, k_i - k_j)$ for a phonon line of momentum q going from quasiparticle line $k_j$ to quasiparticle line $k_i$. (2.10a)

(b) An integration $\int d\ell\,/\,2\pi$ for each closed loop. (2.10b)

For any particular ordering of the $k_i$'s, it is easy to see that (2.10) is equivalent to the rules (2.5) of II. A detailed discussion of the skeleton expansion for N-body wave functions, its physical interpretation, and its connection with Bethe's hypothesis is given in II.

## III. INNER PRODUCTS AND WAVE OPERATOR UNITARITY

The unitarity of the wave operator $U(0, -\infty)$ in (2.1) allows a formal demonstration that the N-particle in state wave functions are orthonormal,

$$\langle \Psi_N^{(+)}(k') | \Psi_N^{(+)}(k) \rangle = \langle k' | U^\dagger(0, -\infty) U(0, -\infty) | k \rangle = \langle k' | k \rangle \ . \qquad (3.1)$$

where $|k\rangle \equiv |k_1, \ldots k_N\rangle$. Explicit verification of (3.1) in terms of factorized graphs involves some intricate cancellations among various sets of graphs. In this section we will develop a systematic graphical procedure for evaluating inner products of the form (3.1) and thereby obtain wave operator unitarity constraints on inner product graphs. These constraints are a crucial ingredient in the calculation of thermodynamic quantities described in Secs. IV and V.

The evaluation of the inner product on the left-hand side of (3.1) is most easily understood by manipulation of graphs. The ket state $|\Psi^{(+)}(k)\rangle$ is represented by a set of factorized graphs with the pseudomomentum of each quasiparticle line determined by the momentum $k_i$ at the bottom of the graph. The bra state $\langle \Psi^{(+)}(k') |$ can be envisioned as a similar set of graphs turned upside down, i.e. with pseudomomentum labels at the top of the graph. The construction of an upside down bra state graph entails both a complex conjugation of all quantities and a reversal of the flow of momentum through all lines. The implied integration over the phase space of the intermediate states $|p\rangle\langle p|$ between $\langle \Psi^{(+)}(k') |$ and $|\Psi^{(+)}(k)\rangle$ is accomplished by joining lines from these two sets of graphs, producing

inner product graphs which have pseudomomentum labels $k_i$ at the bottom and $k'_i$ at the top. This procedure is depicted in Fig. 3. Notice that, by virtue of the symmetrization of the intermediate state over the momenta $p_i$, the quasiparticle lines from the upper and lower graphs must be joined together in all N! possible ways. It is convenient to arrange the lower pseudomomenta $k_i$ in a particular order $k_1, k_2, \ldots k_N$, and classify the inner product graphs according to a permutation P, where $k'_{P_1}, k'_{P_2}, \ldots k'_{P_N}$ is the ordering of the upper pseudomomenta.

Turning to the phonon lines, we note that the skeletal structure of an inner product graph can, in general, be simplified by using the properties of factorized graphs, namely: (1) vertex commutativity, and (2) loop integration by line removal (i.e. Fig. 4). Thus, for example, the skeleton in Fig. 5a reduces to Fig. 5b. A pair of quasiparticle lines in an inner product skeleton graph will be connected by a phonon line if a collision took place in either the bra state or the ket state or both. Thus, in a dressed inner product graph, a phonon line of momentum q which connects two quasiparticle lines labelled $k_i$ and $k_j$ at the bottom and $k'_{P_i}$ and $k'_{P_j}$ at the top will represent the sum of three terms,

$$\Gamma(q; k'_{P_i P_j}, k_{ij}) = \tilde{\Delta}(q; k_{ij}) + \tilde{\Delta}^*(-q; k'_{P_i P_j}) + \int \frac{d\ell}{2\pi} \tilde{\Delta}(\ell; k_{ij}) \tilde{\Delta}^*(\ell - q; k'_{P_i P_j}) \quad . \qquad (3.2a)$$

Explicitly,

$$\Gamma(q;\, k'_{P_iP_j},\, k_{ij}) = \left\{\tau(k_{ji}) + \tau^*(k'_{P_jP_i}) + \tau(k_{ji})\tau(k'_{P_jP_i})\right\}\left(\frac{-i}{q - i\epsilon}\right)$$

$$\text{for } k_{ij} > 0,\ k'_{P_iP_j} > 0 \tag{3.2b}$$

and

$$\Gamma(q;\, k'_{P_iP_j},\, k_{ij}) = \tau(k_{ji})\left(\frac{-i}{q - i\epsilon}\right) + \tau^*(k'_{P_iP_j})\left(\frac{i}{q + i\epsilon}\right)$$

$$\text{for } k_{ij} > 0,\ k'_{P_iP_j} < 0 \quad . \tag{3.2c}$$

The other two sign combinations for $k_{ij}$ and $k_{P_iP_j}$ can be obtained from the symmetry relation

$$\Gamma(q;\, k'_{P_iP_j},\, k_{ij}) = \Gamma(-q;\, k'_{P_jP_i},\, k_{ji}) \quad . \tag{3.3}$$

An N-particle inner product graph is thus completely specified by a permutation $P \in S_N$ and a collision set $\mathscr{C} \in \mathscr{P}(\mathscr{E}_N)$. Such a graph will be denoted $\mathscr{I}_N(k'_{P_1}, \ldots k'_{P_N};\, k_1, \ldots k_N; \mathscr{C}) \equiv \mathscr{I}_N(Pk';\, k;\, \mathscr{C})$. The value of $\mathscr{I}_N(Pk';\, k;\, \mathscr{C})$ is given by the following rules:

(a) Draw N quasiparticle lines with momenta $k_1, k_2, \ldots k_N$ flowing in from the bottom of the graph and $k'_{P_1}, k'_{P_2}, \ldots k'_{P_N}$ flowing out from the top. (3.4a)

(b) For each pair $(i, j) \in \mathscr{C}$, draw a phonon line connecting the quasiparticle lines which are labelled at the bottom by $k_i$ and $k_j$. (3.4b)

(c) For a phonon of momentum q corresponding to $(i, j) \in \mathscr{C}$, write a factor $\Gamma(q; k'_{P_i P_j}, k_{ij})$. (3.4c)

(d) Perform an integration $\int d\ell/2\pi$ over each closed loop. (3.4d)

The left-hand side of (3.1) is given by the sum of all distinct inner product graphs,

$$\langle \Psi_N^{(+)}(k') | \Psi_N^{(+)}(k) \rangle = 2\pi\, \delta\left( \sum_{i=1}^{N} k_i - \sum_{i=1}^{N} k'_i \right) \sum_{P \in S_N} \sum_{\mathscr{C} \in \mathscr{P}(\mathscr{E}_N)} \mathscr{I}_N(Pk'; k; \mathscr{C}) \qquad (3.5)$$

Combining the graphical expansion (3.5) with the constraint (3.1), we obtain wave operator unitarity relations among the inner product graphs $\mathscr{I}_N$. The most useful form of these relations is obtained by a cluster decomposition of the inner product. Let us define the connected part Y of an operator W by

$$\langle 1' | W | 1 \rangle = \langle 1' | Y | 1 \rangle$$

$$\langle 1'2' | W | 12 \rangle = \langle 1' | Y | 1 \rangle \langle 2' | Y | 2 \rangle + \langle 1'2' | Y | 1,2 \rangle$$

$$\langle 1'2'3' | W | 123 \rangle = \langle 1' | Y | 1 \rangle \langle 2' | Y | 2 \rangle \langle 3' | Y | 3 \rangle$$

$$+ \langle 1' | Y | 1 \rangle \langle 2', 3' | Y | 2,3 \rangle$$

$$+ \langle 2' | Y | 2 \rangle \langle 1', 3' | Y | 1,3 \rangle$$

$$+ \langle 3' \,|\, Y \,|\, 3 \rangle \langle 1', 2' \,|\, Y \,|\, 1, 2 \rangle$$

$$+ \langle 1', 2', 3' \,|\, Y \,|\, 1, 2, 3 \rangle, \text{ etc.} \qquad (3.6)$$

Here we use the shorthand

$$|k_1, k_2 \ldots\rangle \rightarrow |1, 2 \ldots\rangle$$

$$|k'_1, k'_2 \ldots\rangle \rightarrow |1', 2' \ldots\rangle \quad . \qquad (3.7)$$

It should be noted that the operator Y defined by (3.6) includes not only those graphs in which all particles are connected by interactions but also graphs in which otherwise disconnected clusters are connected by statistics. For example, the exchange term $\langle 1' \,|\, W \,|\, 2\rangle\langle 2' \,|\, W \,|\, 1\rangle$ would be included in $\langle 1', 2' \,|\, Y \,|\, 1, 2\rangle$. This definition of connectedness is appropriate to the discussion of Hilbert space traces. For some purposes it is desirable to isolate those graphs which are fully connected in the ordinary sense, i.e. by interactions. This is accomplished by defining an operator T by

$$\langle 1' \,|\, Y \,|\, 1\rangle = \langle 1' \,|\, T \,|\, 1\rangle$$

$$\langle 1', 2' \,|\, Y \,|\, 1, 2\rangle = \langle 2' \,|\, T \,|\, 1\rangle\langle 1' \,|\, T \,|\, 2\rangle + \langle 1', 2' \,|\, T \,|\, 1, 2\rangle$$

$$\langle 1', 2', 3' \,|\, Y \,|\, 1, 2, 3\rangle = \langle 1' \,|\, T \,|\, 3\rangle\langle 3' \,|\, T \,|\, 2\rangle\langle 2' \,|\, T \,|\, 1\rangle$$

$$+ \langle 1' \,|\, T \,|\, 2\rangle\langle 2' \,|\, T \,|\, 3\rangle\langle 3' \,|\, T \,|\, 1\rangle$$

$$+ \langle 1' \,|\, \Upsilon \,|\, 2 \rangle \langle 2', 3' \,|\, \Upsilon \,|\, 1, 3 \rangle$$

$$+ \langle 1' \,|\, \Upsilon \,|\, 3 \rangle \langle 2', 3' \,|\, \Upsilon \,|\, 1, 2 \rangle$$

$$+ \langle 2' \,|\, \Upsilon \,|\, 1 \rangle \langle 1', 3' \,|\, \Upsilon \,|\, 2, 3 \rangle$$

$$+ \langle 2' \,|\, \Upsilon \,|\, 3 \rangle \langle 1', 3' \,|\, \Upsilon \,|\, 1, 2 \rangle$$

$$+ \langle 3' \,|\, \Upsilon \,|\, 1 \rangle \langle 1', 2' \,|\, \Upsilon \,|\, 2, 3 \rangle$$

$$+ \langle 3' \,|\, \Upsilon \,|\, 2 \rangle \langle 1', 2' \,|\, \Upsilon \,|\, 1, 3 \rangle$$

$$+ \langle 1', 2', 3' \,|\, \Upsilon \,|\, 1, 2, 3 \rangle, \text{ etc.} \qquad (3.8)$$

Matrix elements of $\Upsilon$ are given by the sum of graphs which are completely connected by interactions. By letting

$$W = U^{\dagger}(0, -\infty) U(0, -\infty) \quad , \qquad (3.9)$$

we obtain a cluster decomposition of the inner product (3.5). Using (3.6) and (3.8), we can write the wave operator unitarity constraint (3.1) as

$$\langle 1', 2', \ldots N' \,|\, \Upsilon \,|\, 1, 2, \ldots N \rangle = 0, \quad N > 1 \quad . \qquad (3.10)$$

From (3.5) and (3.9) we have

$$\sum_{\mathscr{C}}{}' \sum_{P \in S_N} \mathscr{I}_N(Pk'; k; \mathscr{C}) = 0, \quad N > 1 \qquad (3.11)$$

where the primed sum extends over all collision sets describing graphs which are completely connected by phonon lines.

The two-body system serves as an instructive example of the above considerations. For N = 2 there is only one term in the primed sum in (3.11), namely $\mathscr{C} = \{(1, 2)\}$. The sum over permutations gives the two graphs shown in Fig. 6. These are easily evaluated by the rules (3.4). Assuming for definiteness that $k_1 < k_2$ and $k'_1 < k'_2$, we find

$$\mathscr{I}\left(k'_1, k'_2; k_1, k_2; \{(1, 2)\}\right) = \frac{-4c}{(k_{12} - ic)(k'_{12} + ic)} \tag{3.12a}$$

$$\mathscr{I}\left(k'_2, k'_1; k_1, k_2; \{(1, 2)\}\right) = \frac{4c}{(k_{12} - ic)(k'_{12} + ic)} \tag{3.12b}$$

which confirms the result (3.11) for N = 2.

The verification of (3.11) for N > 2 involves a considerable amount of manipulation and regrouping of terms in the sum of inner product graphs. Since a graphical understanding of the unitarity relations is essential to our calculation of thermodynamic quantities, we will discuss these manipulations in some detail. Instead of showing (3.11), we will discuss the slightly weaker constraint

$$\sum \equiv (\omega_k - \omega'_k) \sum_{\mathscr{C}}{}' \sum_{P \in S_N} \mathscr{I}_N(Pk'; k; \mathscr{C}) = 0 \tag{3.13}$$

where $\omega_k$ and $\omega'_k$ are defined as in (2.3). Factorizing energy differences term by term, we get

$$\sum = \sum_{\mathscr{C}}{}' \sum_{P\in S_N} \sum_{i=1}^{N} (k_i^2 - k'^2_{P_i}) \quad \mathscr{I}_N(Pk'; k; \mathscr{C})$$

$$= \sum_{\mathscr{C}}{}' \sum_{P\in S_N} \sum_{i=1}^{N} (k_i + k'_{P_i})(k_i - k'_{P_i}) \quad \mathscr{I}_N(Pk'; k; \mathscr{C}) \; . \qquad (3.14)$$

The inner product graphs are given by the rules (3.4), specifically

$$\mathscr{I}_N(Pk',\ k;\ \mathscr{C}) \;=\; \int \frac{d\ell_1}{2\pi} \cdots \frac{d\ell_L}{2\pi} \prod_{(i,j)\in \mathscr{C}} \Gamma(q_{ij}; k'_{P_i P_j},\ k_{ij}) \qquad (3.15)$$

where L is the number of closed loops and $q_{ij}$ is the momentum carried by the phonon (i, j) defined to flow from line j to line i. The momentum difference in (3.14) is equal to the sum of all momenta flowing into line i, as depicted in Fig. 7,

$$k'_{P_i} - k_i \;=\; \sum_{\{j \,|\, (j,\ i)\in\mathscr{C}\}} q_{ji} \;-\; \sum_{\{\ell \,|\, (i,\ \ell)\in\mathscr{C}\}} q_{i\ell} \qquad (3.16)$$

where the notation implies a sum over all phonons connecting to line i. Inserting (3.15) and (3.16) into (3.14), we find

$$\sum = \sum_{P\in S_N} \sum_{\mathscr{C}}{}' \sum_{(i,j)\in\mathscr{C}} \int \frac{d\ell_1}{2\pi} \cdots \frac{d\ell_L}{2\pi} (k_{ij} + k'_{P_i P_j}) q_{ij}$$

$$\times \prod_{(\ell,m)\in\mathscr{C}} \Gamma(q_{\ell m};\ k'_{P_\ell P_m},\ k_{\ell m}) \qquad (3.1\ )$$

We now separate the (i, j) factor from the product of $\Gamma$'s, writing

$$\prod_{(\ell,m)\in\mathscr{C}} \Gamma(q_{\ell m}; k'_{P_\ell P_m}, k_{\ell m}) = \Gamma(q_{ij}; k'_{P_i P_j}, k_{ij}) \times \prod_{\substack{(\ell,m)\in\mathscr{C} \\ (\ell,m)\neq(i,j)}} \Gamma(q_{\ell m}; k'_{P_\ell P_m}, k_{\ell m}) \quad . \tag{3.18}$$

By noting the explicit form of $\Gamma$, Eq. (3.2), it is seen that

$$q_{ij}\Gamma(q_{ij}; k'_{P_i P_j}, k_{ij}) \equiv \Gamma_0(k'_{P_i P_j}, k_{ij}) \tag{3.19}$$

is independent of $q_{ij}$. It is convenient to represent $\Gamma_0$ in (3.19) by a dashed line connecting quasiparticle lines i and j as shown in Fig. 8. The skeletal structure of an inner product graph containing such a dashed line is completely analogous to that of the "amplitude graphs" used in II. Eq. (3.17) can be written

$$\sum = \sum_{P\in S_N} \sum_{\mathscr{C}}{}' \sum_{(i,j)\in\mathscr{C}} (k_{ij} + k'_{P_i P_j})\Gamma_0(k'_{P_i P_j}, k_{ij}) \times \int \frac{d\ell_1}{2\pi} \cdots \frac{d\ell_L}{2\pi} \prod_{\substack{(\ell,m)\in\mathscr{C} \\ (\ell,m)\neq(i,j)}} \Gamma(q_{\ell m}; k'_{P_\ell P_m}, k_{\ell m}) \tag{3.20}$$

The double sum in (3.20) over $(i,j)\epsilon\mathscr{C}$ and over $\mathscr{C}$ can be thought of as a sum over all possible connected skeletal structures that can be built from N quasiparticle lines, one dashed line, and any number of phonon lines (with no pair of quasiparticle lines being connected more than once). We can invert the order of this double sum, grouping together all those graphs which have a particular pair (i, j) connected by the dashed line, i.e.

$$\sum_{\mathscr{C}}{}' \sum_{(i,j)\epsilon\mathscr{C}} \rightarrow \sum_{(i,j)\epsilon\mathscr{E}_N} \sum_{\mathscr{C}}{}'' \tag{3.21}$$

where $\mathscr{E}_N$ is defined in (2.4), and the double primed sum is over all those connected collision sets which contain the pair (i, j). With the regrouping of terms (3.21), we find

$$\sum = \sum_{(i,j)\epsilon\,\mathscr{E}_N} \sum_{P\epsilon S_N} (k_{ij} + k'_{P_iP_j})\, \Gamma_0(k'_{P_iP_j}, k_{ij}) F_{ij}(Pk', k) \tag{3.22}$$

where

$$F_{ij}(Pk', k) = \sum_{\mathscr{C}}{}'' \int \frac{d\ell_1}{2\pi} \cdots \frac{d\ell_L}{2\pi} \prod_{\substack{(\ell,m)\epsilon\mathscr{C} \\ (\ell,m)\neq(i,j)}} \Gamma(q_{\ell m}; k'_{P_\ell P_m}, k_{\ell m}) \,. \tag{3.23}$$

We will now show that the unitarity constraint $\Sigma = 0$ results from a pairwise cancellation among the terms in the sum over permutations

$P \epsilon S_N$ in (3.22). This is seen by dividing the elements of the permutation group $S_N$ into two subsets,

$$S_N = \sigma_N(i, j) \cup \sigma_N(j, i) \quad , \tag{3.24}$$

where

$$\sigma_N(i, j) = \{ P \in S_N \mid P_i < P_j \} \quad . \tag{3.25}$$

For each permutation $P \in \sigma_N(i, j)$ there is a corresponding permutation $\overline{P} \in \sigma_N(j, i)$, where

$$\overline{P} = P_{ij} P \tag{3.26}$$

and $P_{ij}$ is the permutation which interchanges the ith and jth members of an N-tuple. On a graph this represents the interchange of pseudomomentum labels $k'_{P_i}$ and $k'_{P_j}$. A crucial property of the function (3.23) is its symmetry under this interchange,

$$F_{ij}(\overline{P}k', k) = F_{ij}(Pk', k) \tag{3.27}$$

where $\overline{P}$ and $P$ are related by (3.26). This will be shown explicitly below, but first let us see that it leads directly to the unitarity cancellation. With (3.27), (3.22) becomes

$$\sum = \sum_{(i,j) \in \mathscr{E}_N} \sum_{P \in \sigma_N(i,j)} \Big\{ (k_{ij} + k'_{P_i P_j}) \Gamma_0(k'_{P_i P_j}, k_{ij}) + (k_{ij} + k'_{P_j P_i}) \Gamma_0(k'_{P_j P_i}, k_{ij}) \Big\} F_{ij}(Pk', k) \quad . \tag{3.28}$$

The result $\Sigma = 0$ now follows easily, because the quantity in curly brackets vanishes identically, as can be seen by inspection of (3.2) and (3.19). This is in fact a revisitation of the unitarity cancellation in the two-body problems, Eq. (3.12).

The symmetry relation (3.27) can be understood by considering the graphical structure of $F_{ij}$. In changing P to $\overline{P}$ in (3.23), we interchange $k'_{P_i}$ and $k'_{P_j}$. This affects only those factors in the integrand which correspond to phonons connecting to quasiparticle line i or j. Another quasiparticle line m may be connected by phonon(s) to line i or j or both. In the last case the two phonons form a closed loop. Thus, when the sum over $\mathscr{C}$'s in (3.23) is carried out under the integral sign, the factors in the integrand which are relevant to the proof of (3.27) take the form

$$\Gamma(q; k'_{P_i P_m}, k_{im}) + \Gamma(q; k'_{P_j P_m}, k_{jm})$$

$$+ \int \frac{d\ell}{2\pi} \Gamma(\ell; k'_{P_i P_m}, k_{im}) \Gamma(q - \ell; k'_{P_j P_m}, k_{jm}) \quad . \tag{3.29}$$

This expression can be shown to be symmetric under the interchange $k_{P_i} \leftrightarrow k_{P_j}$ by simply inserting (3.2a) in (3.29) and inspecting terms.

## IV. GRAPHICAL THEORY OF STATISTICAL MECHANICS

We will review briefly the operator formulation of statistical mechanics discussed in II. The N-particle partition function can be written as a contour integral in the complex energy plane with an integrand involving the trace of the resolvent operator of the hamiltonian H. By closing the contour around the real energy axis we obtain

$$Q_N = Tr_N(e^{-\beta H}) = \int_0^\infty \frac{dE}{2\pi i} e^{-\beta E} Tr_N\{G(E - i\epsilon) - G(E + i\epsilon)\} \quad . \qquad (4.1)$$

Here, the limit $\epsilon \to 0$ is understood to be taken at the end of the calculation. The delicacy of this limit forms the main subject of this section. We can expand the operators $G(E \pm i\epsilon)$ in (4.1) as a perturbation series,

$$G = G_0 + G_0 V G_0 + \ldots \qquad (4.2)$$

In order to evaluate (4.1) via the graphical scattering theory formalism already developed, we use the cyclic property of the trace to get

$$Q_N = \int_0^\infty dE e^{-\beta E} Tr_N \{\delta(E - H_0)\Omega^\dagger(E + i\epsilon)\Omega(E + i\epsilon)\}$$

$$= \frac{1}{N!} \int \frac{dk_1}{2\pi} \cdots \frac{dk_N}{2\pi} \exp\left\{-\beta \sum_{i=1}^{N} k_i^2\right\} \langle k_1 \ldots k_N | W_\epsilon | k_1 \ldots k_N \rangle \qquad (4.3)$$

where $\delta(E - H_0)$ is an operator delta function, and

$$\Omega(E + i\epsilon) = \sum_{n=0}^{\infty} \left[G_0(E + i\epsilon)V\right]^n \quad . \tag{4.4}$$

The operator $W_\epsilon$ is defined by

$$\langle k'_1 \ldots k'_N | W_\epsilon | k_1 \ldots k_N \rangle = \langle k'_1 \ldots k'_N | \Omega^{\dagger}(\omega'_k + i\epsilon)\Omega(\omega_k + i\epsilon) | k_1 \ldots k_N \rangle \ , \tag{4.5}$$

with

$$\omega_k \equiv \sum_{i=1}^{N} k_i^2 \quad . \tag{4.6}$$

The subscript $\epsilon$ is meant to denote the manner in which the diagonal (forward) matrix elements of $W_\epsilon$ are computed. This calculation involves the following sequence of limits: (referred to below as the "thermodynamic limit"): (1) $k'_i \to k_i$, followed by (2) $\epsilon \to 0$. From (4.4) and (4.5) we find the formal result

$$W_\epsilon \xrightarrow[\epsilon \to 0]{} W \tag{4.7}$$

where W is defined in (3.9 ). However, the forward matrix elements of W are computed by the prescription (referred to below as the "forward scattering limit"): (1) $\epsilon \to 0$, followed by (2) $k'_i \to k_i$. The $\epsilon \to 0$ and $k'_i \to k_i$ limits do not commute, and hence $W_\epsilon \neq W$ (W is in fact unity whereas $W_\epsilon$ contains all thermodynamic information).

These points are well illustrated by the calculation of the second virial coefficient,[2] which will also serve to introduce the more general results. The part of the two body partition function which depends on the interaction is obtained from the thermodynamic limit of two graphs, Figs. 6a and 6b. Assuming for convenience that $k_1 < k_2$ and $k'_1 < k'_2$, they are given respectively by

$$\Gamma_\epsilon(k_1 - k'_1; k'_{21}, k_{21}) = \frac{-4c}{(k_{21}+ic)(k'_{21}-ic)} \left(\frac{k_{12}-k'_{12}}{k_{12}-k'_{12}-i\epsilon}\right) \tag{4.8a}$$

$$\Gamma_\epsilon(k_1 - k'_2; k'_{12}, k_{21}) = \left(\frac{4c}{k_{12}-ic}\right)\left(\frac{1}{k_{12}+k'_{12}-i\epsilon}\right) + \left(\frac{4c}{k'_{12}+ic}\right)\left(\frac{1}{k_{12}+k'_{12}+i\epsilon}\right) \tag{4.8b}$$

In (4.8b), the $\epsilon \to 0$ and $k'_i \to k_i$ limits commute. Thus,

$$\lim_{\epsilon \to 0} \lim_{k'_i \to k_i} \Gamma_\epsilon(k_1 - k'_2; k'_{12}, k_{21}) = \lim_{k'_i \to k_i} \lim_{\epsilon \to 0} \Gamma_\epsilon(k_1 - k'_2; k'_{12}, k_{21})$$

$$= \frac{4c}{k_{12}^2 + c^2} - 4\pi\delta(k_{12}) \equiv 2\Delta_0(k_{12}) \quad . \tag{4.9}$$

The forward scattering limit of (4.8a) is $-2\Delta_0(k_{12})$ and just cancels (4.9) as required by wave operator unitarity. On the other hand, the thermodynamic limit of (4.8a) vanishes,

$$\lim_{\epsilon \to 0} \lim_{k'_i \to k_i} \Gamma_\epsilon(k_1 - k'_1; k'_{21}, k_{21}) = 0 \quad . \tag{4.10}$$

The non-commutativity of the thermodynamic and forward scattering limits of (4.8a) results from the fact that the momentum carried by the phonon in Fig. 6a is forced to vanish when $k'_i \to k_i$. (A phonon with this property will be called "infrared".) These results can be understood from a more general point of view. A momentum pole, represented graphically by a phonon, can be associated with a semi-infinite integration in configuration space. This integration is damped by an oscillating factor $e^{iqx}$ where q is the phonon momentum. Infrared phonons arise from the asymptotic parts of the wave function where the integration becomes undamped when $k'_i \to k_i$. But potential infrared terms of $O(q^{-1})$ always vanish (after non-interacting parts of the inner product are subtracted off) because the phase shifts of the bra and ket states "match up" producing a forward zero of the form $(e^{i(\Theta - \Theta')} - 1)$. The vanishing of (4.10) exemplifies this general result. The unitarity cancellation in the forward scattering limit occurs between the $O(q^0)$ part of the infrared graph Fig. 6a and the (unambiguous) forward limit of the non-infrared graph, Fig. 6b. The second virial coefficient can therefore be calculated directly from the forward scattering limit of the infrared graph (See II).

The extension of this analysis to $N > 2$ follows from the wave operator unitarity results of Sec. III. The quantity $\Delta_0(k)$ in (4.9) occurs frequently and will be called a "0-phonon" propagator. It is depicted in Fig. 9. By the foregoing discussion, a 0-phonon can be interpreted as the $q \to 0$ limit of an infrared phonon. We will find that forward matrix elements

of $W_\epsilon$ can be evaluated by graphs constructed from 0-phonons and quasiparticle lines. Let us define a phonon tree graph as one which falls into two disconnected pieces by the removal of any phonon line. We include both statistical and dynamical connectedness as part of this designation, e.g. Fig. 6a is a phonon tree, but Fig. 6b is not. Defining $Y_\epsilon$ from $W_\epsilon$ in precise analogy with Eq. (3.6), we find that

$$\langle k_1,\ldots,k_N | Y_\epsilon | k_1,\ldots,k_N\rangle = \sum\{\text{all connected 0-phonon tree graphs}\} \qquad (4.11)$$

where each 0-phonon incurs a factor

$$\Delta_0(k_{ij}) = \frac{2c}{k_{ij}^2 + c^2} - 2\pi\,\delta(k_{ij}) \quad . \qquad (4.12)$$

The demonstration of (4.11) proceeds by an inductive argument which will be sketched here. We choose a fixed set of $k_i$'s and study matrix elements near the forward direction $k'_i \to k_i$. It is convenient to define two quantities,

$$Y(q) = \langle k_1 - (N-1)q,\ k_2 + q,\ \ldots,\ k_N + q | Y | k_1, k_2, \ldots, k_N\rangle \qquad (4.13)$$

where Y is defined by (3.9) and (3.6), and

$$Y_\epsilon(q) = \frac{1}{N}\langle k_1+q, k_2+q,\ldots,k_N+q | U^\dagger(0,-\infty) j_0(Nq) U(0,-\infty) | k_1,\ldots,k_N\rangle_{\text{conn}} \qquad (4.14)$$

where $j_\theta$ is the charge density operator in momentum space.

$$j_0(q) = \int \frac{dp}{2\pi} a^+_{p+q} a_p \quad . \tag{4.15}$$

These two quantities are depicted in Figs. 10a and 10b respectively. The result (4.11) is a consequence of the following assertions:

$$\lim_{q \to 0} Y_\epsilon(q) = \langle k_1, \ldots, k_N | Y_\epsilon | k_1, \ldots, k_N \rangle \tag{4.16}$$

$$Y(q) = 0, \quad q \neq 0 \tag{4.17}$$

$$\lim_{q \to 0} \left[ Y_\epsilon(q) - Y(q) \right] = \sum \{ \text{all connected 0-phonon tree graphs} \} \quad . \tag{4.18}$$

Eq. (4.16) follows from the cancellation of infrared singularities in the sum of inner product graphs. As discussed previously, an infrared phonon pole $(q - i\epsilon)^{-1}$ will be multiplied by a vanishing phase shift factor

$$e^{i(\Theta - \Theta')} - 1 \tag{4.19}$$

where $\Theta' \to \Theta$ as $q \to 0$. But the phase shifts $\Theta$ and $\Theta'$ are Galilean invariant, i.e. they depend only on momentum differences $k_{ij}$ and $k'_{ij}$ respectively. Thus, factors like (4.19) are identically zero for both the left- and right-hand sides of (4.16). The graphs which do contribute to (4.16) are entirely non-singular and hence give the same result for both sides. Eq. (4.17) is just the statement of wave operator unitarity. Finally, Eq. (4.18) can be shown inductively by noting that the calculation of the first term on the left-hand side differs from that of the second only in the treatment of infrared phonons which connect particle 1 to the

rest of the graph. For $Y_\epsilon(q)$, the sum of such infrared graphs is identically zero due to factors like (4.19). On the other hand, $Y(q)$ is calculated by retaining the $O(q^0)$ terms of the infrared graphs. This is easily found to give a sum of all possible 0-phonon insertions connecting particle 1 to the rest of the graph, with the 0-phonon "propagators" $\Delta_0(k_{ij})$ arising as phase shift derivatives. Eq. (4.18) then follows by induction.

## V. THE EQUATION OF STATE

The equation of state of the system can be obtained from the log of the grand partition function

$$\log \mathcal{Q} = \sum_{N=1}^{\infty} z^N Q_{Nc} \tag{5.1}$$

where $z = e^{\beta\mu}$ = fugacity, $\mu$ = chemical potential, $\beta = (k_B T)^{-1}$, $T$ = temperature, and $Q_{Nc}$ is the connected part of the N-body partition function,

$$Q_{Nc} = \frac{1}{N!} \int dk_1 \ldots dk_N \exp\left\{-\beta \sum_{i=1}^{N} k_i^2\right\} \langle k_1 \ldots k_N | Y_\epsilon | k_1 \ldots k_N \rangle \ . \tag{5.2}$$

With the ansatz (4.11), the only remaining problems involve the counting and summation of graphs. Let us write the permutation P for each 0-phonon graph in $Y_\epsilon$ in its cyclic form (e.g. (P) = (2143) is written (12)(34)), and focus on the $\ell$-cycle which contains particle 1, say

$(1c_2c_3\ldots c_\ell)$. We can collect together all graphs (for all values of N) for which particle 1 is in a 1-cycle (i.e. $P_1 = 1$). Multiplying by $\exp\left\{-\beta \sum_{i=1}^{N} k_i^2\right\}$ and integrating over $k_2, k_3, \ldots k_N$, we obtain an important one-particle distribution function $\zeta(k_1)$, which will be represented by the shaded blob in Fig. 11. In a similar way, those graphs in which particle 1 belongs to an $\ell$-cycle can be contracted over all k's except $k_1, k_{c_2}, \ldots, k_{c_\ell}$, giving the product of $\zeta$'s shown in Fig. 12. This product entails a symmetry factor $(\ell!)^{-1}$. There are $(\ell-1)!$ distinct $\ell$-cycles, and hence the overall symmetry factor for the corresponding term in the equation of state is $\ell^{-1}$. In this way we find an expression for the pressure,[6] Fig. 13

$$\mathcal{P} = \frac{1}{2\pi\beta\,\delta(0)} \log \mathcal{Q}$$

$$= \frac{1}{2\pi\beta} \int dk \sum_{\ell=1}^{\infty} \frac{1}{\ell} \left[\zeta(k)\right]^{\ell}$$

$$= -\frac{1}{2\pi\beta} \int dk \log\left[1 - \zeta(k)\right] \quad . \tag{5.3}$$

The graphical summation involved in the calculation of $\zeta(k)$ can be reduced to an integral equation. The graphs for $\zeta(k)$ can be classified according to the number of 0-phonons attached to the quasiparticle line k, as shown in Fig. 14. A graph with n such phonons contains a symmetry factor $(n!)^{-1}$ associated with the commutativity of vertices and resulting

symmetry of the graph under interchange of phonon labels. Thus $\zeta(k)$ can be written

$$\zeta(k) = e^{-\beta(k^2-\mu)} \sum_{n=0}^{\infty} \frac{1}{n!} \left[-\beta\pi(k)\right]^n$$

$$= \exp\left\{-\beta\left[k^2 + \pi(k) - \mu\right]\right\} \quad . \tag{5.4}$$

Here $\pi(k)$ is essentially the single phonon graph, Fig. 15, and can be interpreted as the quasiparticle self-energy due to the interaction. The end of the phonon line in Fig. 15 which intrudes into the crosshatched blob attaches to a quasiparticle line of momentum k'. The combinatorics and attendant symmetry factors for the remainder of the graph are completely analogous to the derivation of (5.3). The resulting equation[6] for $\pi(k)$ is depicted in Fig. 16,

$$\pi(k) = \frac{1}{\beta} \int \frac{dk'}{2\pi} \Delta_0(k-k') \log\left\{1 - e^{-\beta\left[k'^2+\pi(k')-\mu\right]}\right\} \quad . \tag{5.5}$$

Notice that as $c \to 0$, $\pi(k) \to 0$, and for $c \to \infty$,

$$\pi(k) = -\frac{1}{\beta} \log\left\{1 - e^{-\beta\left[k^2+\pi(k)-\mu\right]}\right\} \quad . \tag{5.6}$$

Thus we obtain a well-known result that the pressure

$$\mathscr{P} = -\frac{1}{2\pi\beta} \int dk \log\left\{1 - e^{-\beta\left[k^2+\pi(k)-\mu\right]}\right\} \tag{5.7}$$

reduces to that of an ideal Bose (Fermi) gas in the limit $c \to 0$ ($c \to \infty$).

## ACKNOWLEDGMENTS

I would like to thank C. N. Yang and R. B. Pearson for discussions.

## FOOTNOTES AND REFERENCES

[1] H. B. Thacker, Phys. Rev. D11, 838 (1975) (hereafter referred to as I).

[2] H. B. Thacker, Phys. Rev. D14, 3508 (1976) (hereafter referred to as II).

[3] C. N. Yang, Phys. Rev. Lett. 19, 1312 (1967); Phys. Rev. 168, 1920 (1968).

[4] J. B. McGuire, J. Math. Phys. 5, 622 (1964).

[5] E. H. Lieb and W. Liniger, Phys. Rev. 130, 1605 (1963); E. H. Lieb, ibid. 130, 1616 (1963).

[6] C. N. Yang and C. P. Yang, J. Math. Phys. 10, 1115 (1969).

[7] E. Brezin and J. Zinn-Justin, C. R. Acad. Sci. (Paris) B263, 670 (1966).

[8] C. N. Yang, in Critical Phenomena in Alloys, Magnets, and Superconductors, edited by R. E. Mills, E. Ascher, and R. I. Jaffe (McGraw Hill, New York, 1971).

[9]See for example K. Huang, Statistical Mechanics (Wiley, New York, 1963), Appendix A.

[10]H. A. Bethe, Z. Phys. 71, 205 (1931).

[11]M. L. Goldberger, Phys. Fluids 2, 252 (1959).

[12]R. Dashen, S. Ma, and H. J. Bernstein, Phys. Rev. 187, 345 (1969).

[13]R. Dashen and S. Ma, J. Math. Phys. 11, 1136 (1970); 12, 689 (1971).

[14]L. D. Landau, Zh. Eksp. Teor. Fiz. 35, 97-103 (July, 1958)[Sov. Phys.-JETP 35 (8), 70 (1959)].

FIGURE CAPTIONS

Fig. 1: Example of a factorized wave function graph.

Fig. 2: (a) A three-body skeleton graph.

(b) The same graph reduced to standard form by repeated use of the identity shown in Fig. 4.

Fig. 3: Construction of an inner product from two sets of wave function graphs.

Fig. 4: An identity used in the reduction of skeleton graphs (c.f. Eq. (2.9) of II).

Fig. 5: (a) Contraction of two wave function skeleton graphs to form an inner product skeleton graph.

(b) Reduction of the inner product skeleton graph.

Fig. 6: (a) Two-body inner product graph with P = (12) = identity.

(b) Two-body inner product graph with P = (21).

Fig. 7: Illustration of Eq. (3.16) for net momentum transfer to a quasiparticle line.

Fig. 8: Graphical representation of $\Gamma_0(k'_{P_i P_j}; k_{ij})$, Eq. (3.19).

Fig. 9: Graphical representation of the 0-phonon propagator, Eq. (4.12).

Fig. 10: (a) The function Y(q), Eq. (4.13).

(b) The function $Y_\epsilon(q)$, Eq. (4.14).

Fig. 11: The distribution function $\zeta(k)$.

Fig. 12: Products of $\zeta(k)$ functions which arise in the calculation of the pressure, Eq. (5.3).

Fig. 13: Summation of "vacuum" graphs, giving the pressure, Eq. (5.3).

Fig. 14: Classification of graphs for $\zeta(\mathbf{k})$ by the number of 0-phonons attaching to quasiparticle line k.

Fig. 15: The quasiparticle self-energy $\pi(k)$.

Fig. 16: Integral equation for the self-energy.

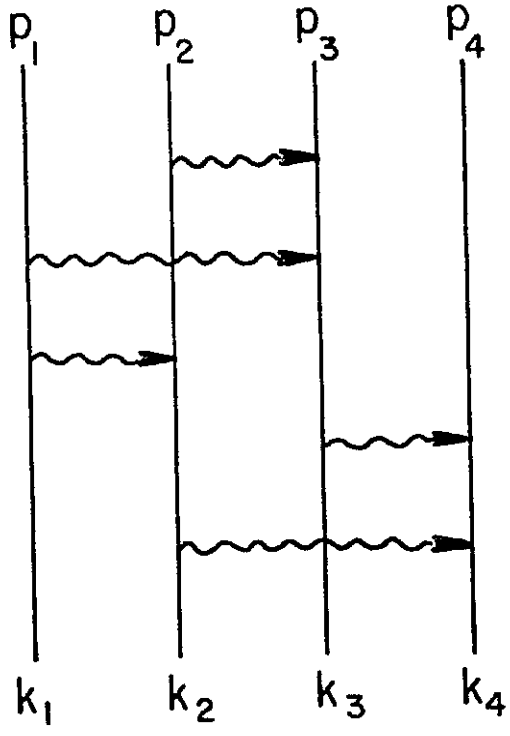


Fig. 1

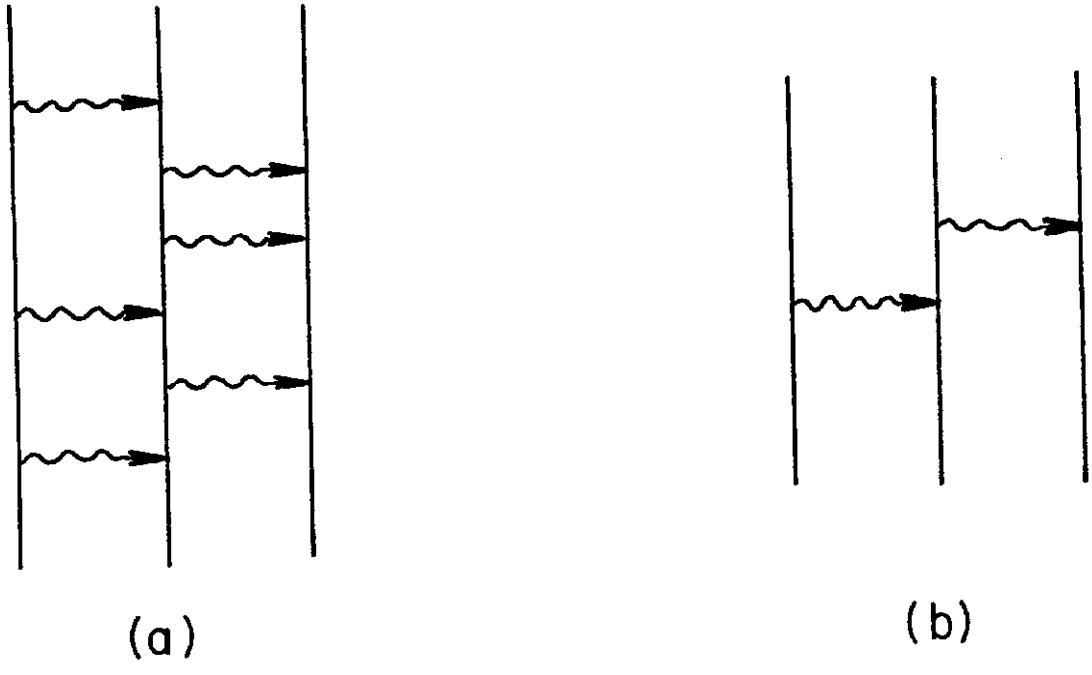


Fig. 2

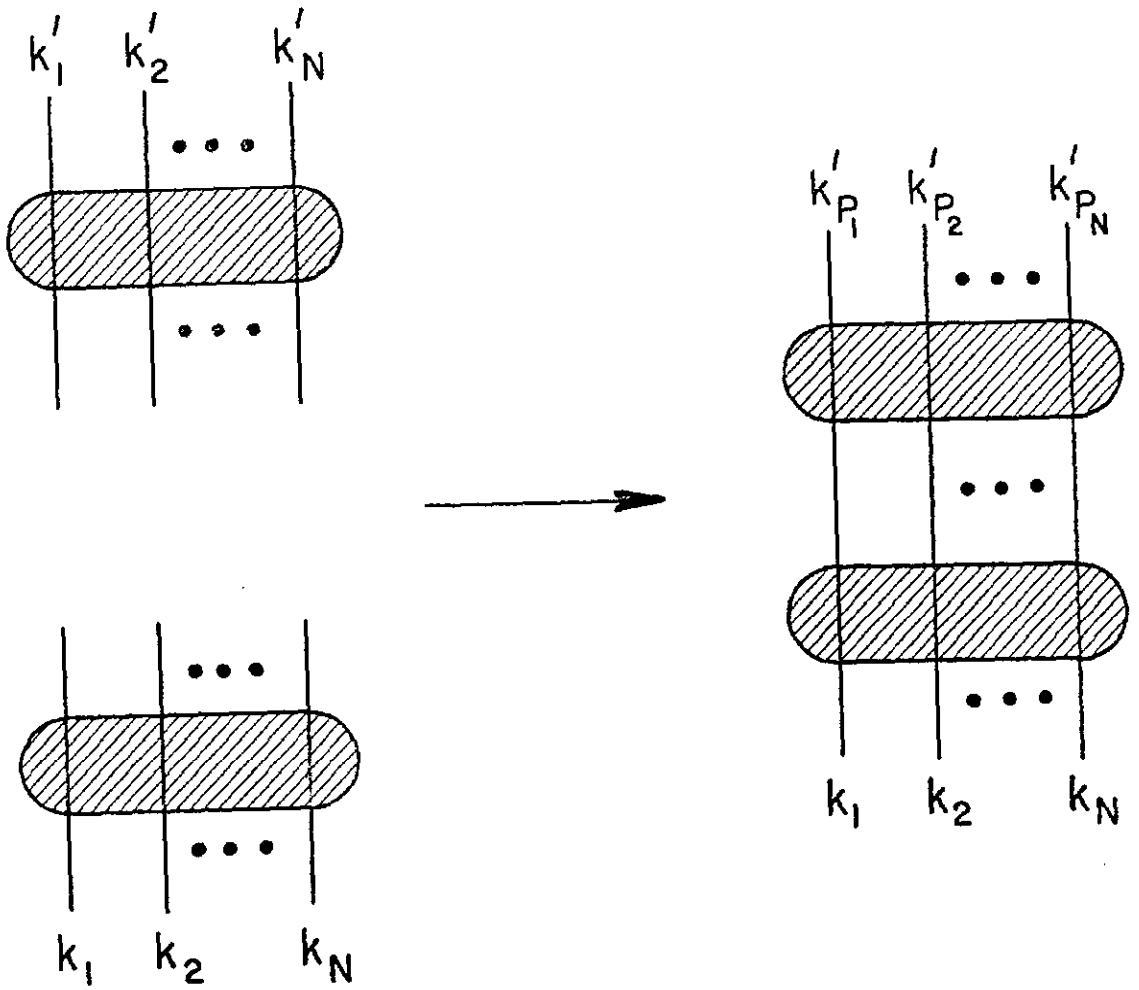


Fig. 3

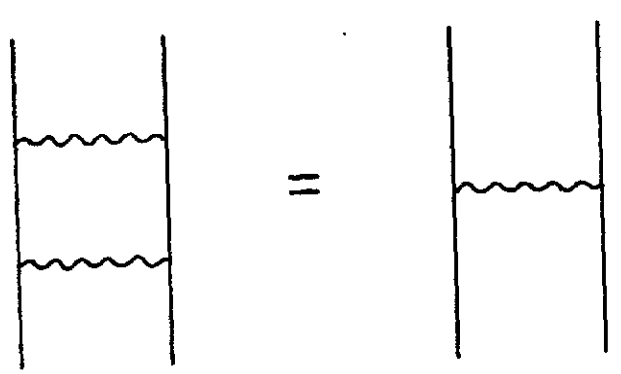

Fig. 4

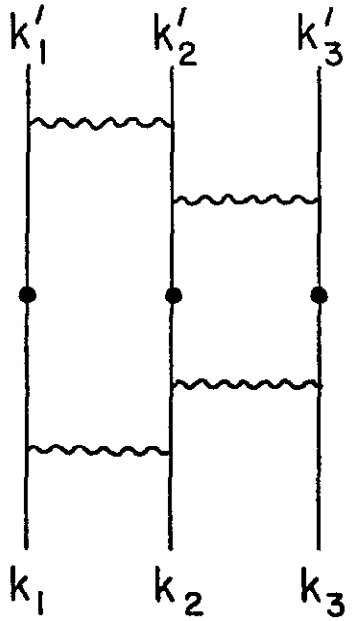


(a)

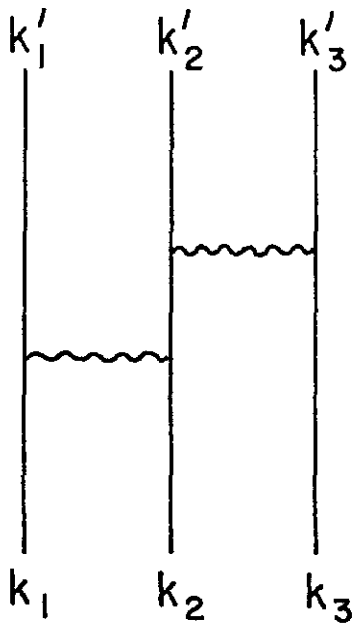


(b)

Fig. 5

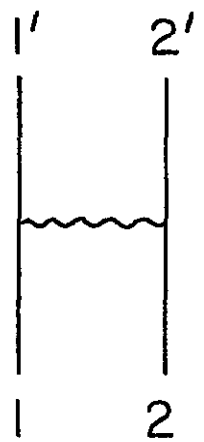


(a)

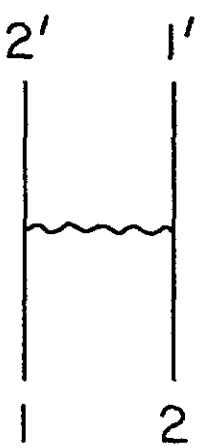


(b)

Fig. 6

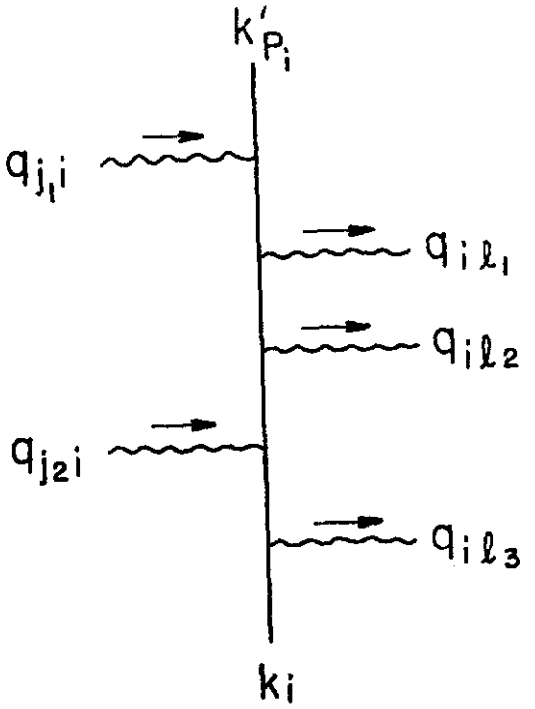


Fig. 7

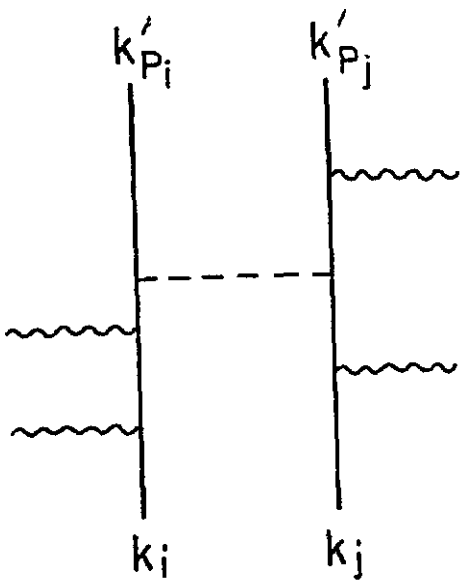


Fig. 8

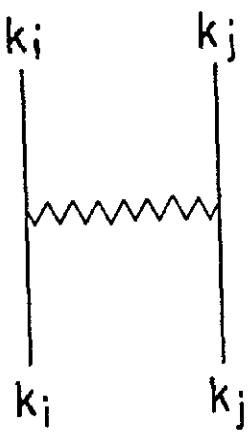


Fig. 9

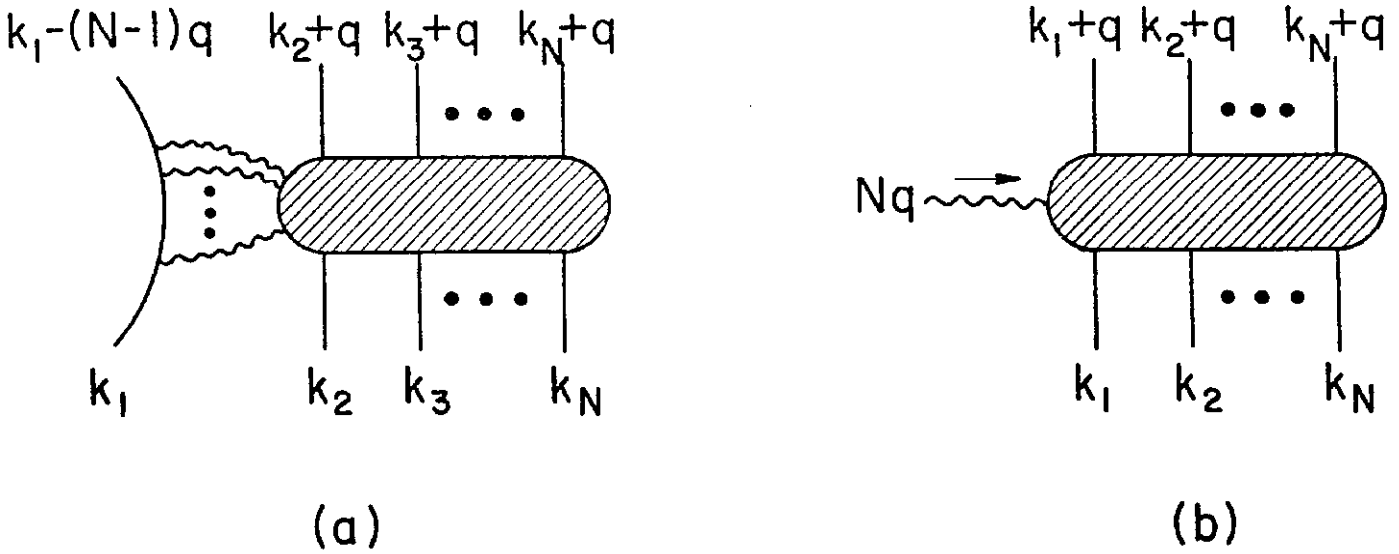


Fig. 10


Fig. 11

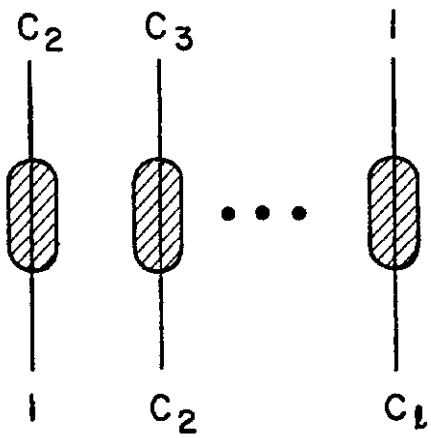


Fig. 12

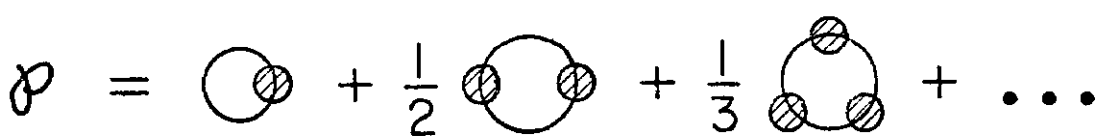


Fig. 13

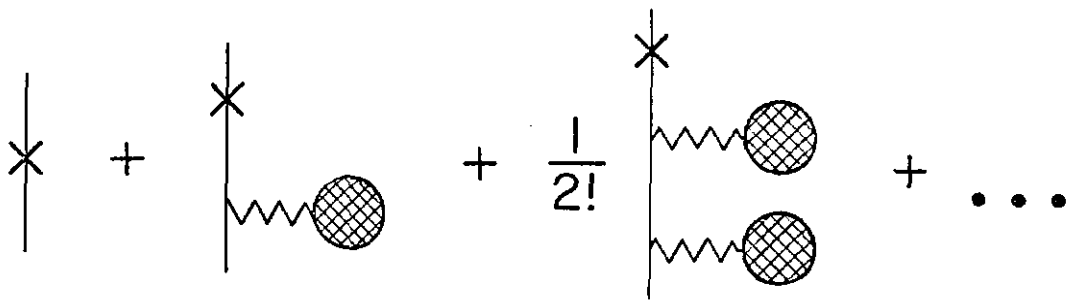

Fig. 14

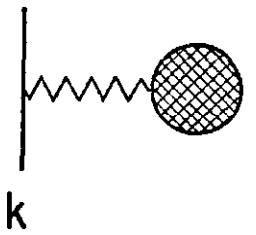


Fig. 15

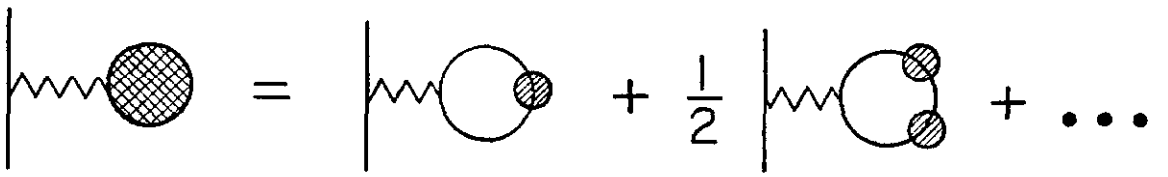

Fig. 16